Supplementary Materials for

COX-2 Inhibition Potentiates Anti-Angiogenic Cancer Therapy and Prevents Metastasis in Preclinical Models

Lihong Xu, Janine Stevens, Mary Beth Hilton, Steven Seaman, Thomas P. Conrads, Timothy D. Veenstra, Daniel Logsdon, Holly Morris, Deborah A. Swing, Nimit L. Patel, Joseph Kalen, Diana C. Haines, Enrique Zudaire, and Brad St. Croix*

*Corresponding author: E-mail: stcroix@ncifcrf.gov

This PDF file includes:

MATERIALS AND METHODS

Study design. The goal of this study was to better understand the mechanism of resistance to VEGF pathway blockade. After we discovered the potential role of the COX-2/PGE_2 pathway in this process, a later goal was to determine the therapeutic potential of simultaneously targeting both the VEGF/VEGFR2 and COX-2/PGE_2 pathways. We chose CT26 cells as a model to identify VEGF-independent angiogenesis mechanisms because in our initial studies these tumors appeared insensitive to VEGF pathway blockade. The Ca^{2+} reporter assay was used to guide the biochemical purification of PGE_2 from the crude heterogeneous mixture of biomolecules in the supernatant of CT26 cells. The crude samples were run over various chromatographic columns and eluted in partially purified fractions that were then evaluated for Ca^{2+} mobilizing activity. After several rounds of chromatographic purification and upon identification of a single chromatographic peak of biochemical activity, the purified sample was considered homogenous and subjected to electrospray ionization mass spectrometry. Encouraged by our initial COX-2/PGE_2 validation studies, we subsequently sought to evaluate the role of COX-2/PGE_2 inhibitors in potentiating the anti-angiogenic activity of VEGF pathway blockers using a variety of tumor and metastasis models. Subcutaneous and orthotopic (mammary fat pad) tumors were measured with digital calipers, whereas metastases were quantified by bioluminescence imaging. All studies were repeated twice. For the survival

studies, we defined death as the time point when moribund animals were euthanized.

Animals. Mice were housed in a pathogen-free facility certified by the Association for Assessment and Accreditation of Laboratory Animal Care International, and the study was carried out in accordance with protocols approved by the NCI Animal Care and Use Committee.

Statistical Analysis

Prior to statistical analysis, groups were tested for Gaussian distribution using the method of Kolmogorov-Smirnov. Groups that followed a Gaussian distribution were subjected to parametric tests (analysis of variance with Bonferroni correction for differences among three or more groups; unpaired Student's t test for differences between two groups). Groups that did not follow a Gaussian distribution were tested by nonparametric tests [Kruskal-Wallis test (nonparametric analysis of variance) with Dunn's correction for differences among groups; Mann-Whitney test for differences between two groups]. For Kaplan Meier survival analysis, a Log-rank (Mantel-Cox) test was used to compare each of the arms. Correlation coefficients were calculated using the Pearson test. Differences between two groups were presented as the mean ± SEM or mean ± SD as noted in the figure legends. All tests were two-sided and p values <0.05 were considered statistically significant. All statistical analysis was performed with GraphPad Prism 6.04.

Cell lines, Vectors and Chemicals. 4T1-luc cells were a kind gift from Dr. P. Charles Lin, HCT116 cells and HCT116/VKO cells were a kind gift from Dr. Long Dang, and CT26 cells were obtained from the ATCC. All cells were maintained in DMEM supplemented with 10% FBS. Luciferase-tagged HCT116-luc and CT26-luc cells were generated by stable transfection of HCT116 and CT26 cells with the pGL4.51 expression vector (Promega) encoding a CMV-driven luciferase reporter codon-optimized for mammalian expression. A COX-2 mammalian expression vector, called pLVX-IRES-tsTomato-COX2, was generated by cloning the human COX-2 gene between EcoR1 and XbaI in the polylinker of pLVX-IRES-tdTomato (Clontech). The COX-2 gene was recovered from a full length IMAGE clone (clone ID: 3880850) using an endogenous EcoR1 site upstream of the "ATG" start codon and incorporating an XbaI site immediately after the "TAG" stop codon using PCR. The VEGF mammalian expression vector, called pLVX-IRES-tsTomato-VEGF, was generated by subcloning murine $VEGF_{164}$ (Addgene; plasmid 10909) cDNA into pLVX-IRES-tdTomato (Clontech). The entire VEGF coding region was PCR amplified using a forward primer that incorporated an EcoR1 site followed by the human Kozak sequence "CCGCCCGCCGCCACC" immediately prior to the "ATG" start codon, and a reverse primer that incorporated a BamH1 sequence immediately after the "TGA" stop codon. The double digested VEGF amplicon was then cloned between the EcoR1/BamH1 sites of pLVX-IRES-tdTomato to create pLVX-IRES-tsTomato-VEGF. The COX-2 and VEGF cDNA expression vectors were sequenced to ensure that they were mutation-free and used to create lentiviral particles using the Lenti-X Lentiviral

expression systems (Clontech). HCT116/VKO cells were infected with lentivirus particles to generate the stable HCT116/VKO sublines. Chemically synthesized PGA_2 and PGE_2 were from Cayman Chemical.

ELISAs. Prostaglandin E_2, prostaglandin D_2, prostaglandin I_2, prostaglandin $F_{2\alpha}$, and thromboxane A_2 were quantified using commercially available kits (Cayman Chemical). Because thromboxane A_2 and prostaglandin I_2 undergo rapid non-enzymatic hydrolysis, concentrations of these prostanoids were estimated based on the more stable metabolites thromboxane B_2 and keto $PGF_{1\alpha}$. VEGF was measured using a VEGF immunoassay (R&D Systems). Tumor tissues were lysed in TNT buffer [50 mM Tris-HCl (pH7.5), 150 mM NaCl, 1% Triton-X100 plus protease inhibitor cocktail (Roche)] and diluted 20-fold prior to ELISA. ELISA values were normalized to tissue protein concentration.

Calcium Assay. Reporter cells (a 293 clone stably transfected with G-alpha16) or control 293 parent cells were plated onto a 96-well plate overnight. A NOVOstar plate reader (BMG Labtech) with an integrated pipetting system was used to transfer conditioned medium from CT26 cells or CT26 clones, biochemically purified fractions, or pure PGA_2 or PGE_2 from a 96-well reagent plate to the 96-well reporter plate. Calcium fluxes were monitored using the Calcium 3 Assay Kit (Molecular Devices) according the manufacturer's recommended protocol.

HPLC and Mass Spectrometry. 10 liters of medium were harvested from CT26 cells grown in RPMI containing 0.5% fetal bovine serum. Medium was filtered through a 5000 MWCO Centricon Plus-80 filter (Amicon), and passed 4 times over an Oasis HLB column (Waters) washing with 50% methanol (MeOH) and eluting with 100% MeOH between each round. Next, the eluate was passed over a series of columns, and a small sample of each eluted fraction was tested for Ca^{2+}-mobilizing activity. Active fractions were pooled and reapplied to the next column. First, the active material was captured on a Delta-Pak C4 column (Waters) in buffer A [5% acetonitrile (ACN), 15% MeOH and 0.1% formic acid] and eluted with an increasing gradient (22-35%) of buffer B (85% ACN, 15% MeOH and 0.065% formic acid). Ca^{2+}-active fractions were then captured on a PRP-1 (Polymeric Reversed Phase) HPLC column (Hamilton) in buffer A, and eluted with a 21-31% gradient of buffer B. Ca^{2+}-active fractions were then run twice over a Delta-Pak C18 column (Waters) in buffer A, eluting from the first column with a 33-43% gradient of buffer B, and from the second column with a 32-39% gradient of buffer B. The most active fraction from peak A (fraction 37) and peak B (fraction 60) (Figure 1E) obtained from the final C18 HPLC fractionation were analyzed using electrospray ionization tandem mass spectrometry (LCQ, ThermoFisher Scientific) by direct infusion.

Tumor Cell Spheroid Formation. Tumor cell spheroids were produced by the liquid overlay method (*41*) with some modifications. Briefly, 24-well plates were coated with 250 µL/well of low melting temperature agarose gel (1%, SeaPlaque Agarose, Cambrex BioScience). 2 x 10^4 cells suspended in 1 mL of culture medium were placed on top of the agarose and allowed to aggregate into a sphere for 48 hours. Cell spheroids were rinsed twice with PBS prior to use in the corneal assay. One spheroid was implanted into each eye.

Mouse Corneal Micropocket Assay. The corneal micropocket assay was performed as previously described, with some modifications (*42*). Briefly, spheroids or pellets containing 160 ng of VEGF were implanted into a corneal incision that was 1.0-1.2 mm (pellet) or 0.6-0.8 mm (spheroids) from the limbus. Ophthalmic erythromycin ointment was used immediately to seal the open pocket and administered for 3 days to prevent infection. Eyes were imaged 5-14 days after implantation. Vasculature area was calculated by the formula $VA=0.02\pi$ x VL x CH where VA is the vessel area (mm^2), VL the longest vessel length (in tenths of millimeters) and CH represents clock hours. Each study contained at least 5 mice per group. All treatments [DC101 (40 mg/kg i.p.), celecoxib (1000 mg/kg of feed), or axitinib (12.5 mg/kg by gavage)] were started the same day the procedure was performed.

Aortic ring sprouting assay. Aortas were excised immediately after sacrifice from 8-12 week-old female Balb/c mice. All extraneous fat, tissue and branching vessels were removed under a dissection microscope on ice. The clean aortae

were cut into rings ~0.5 mm in width and rinsed 3 times with cold PBS. The rings were then embedded in a 1 mg/mL collagen I gel (Millipore) in a 96-well plate, with the luminal axis perpendicular to the well bottom. PGE_2, VEGF or conditioned media were added to the well in a final volume of 150 μL of FBS-free EBM medium (Lonza). The medium was refreshed every other day. After 5 days, microvessel outgrowth was photographed and quantified as described (*43*). Only sprouts attached to the rings were counted.

Matrigel Plug assay. 400 μL of Matrigel (BD Bioscience) mixed with vehicle or PGE_2 (Cayman) on ice were injected subcutaneously into athymic nude mice (one plug per mouse). 7 days later, plugs were removed, photographed, and subjected to a freeze-thaw cycle. The Matrigel was dissolved in Drabkin's reagent (Sigma), and hemoglobin was quantified on a spectrophotometer by comparing the absorption at 540 nM with a pure hemoglobin standard.

RT-PCR. mRNA was purified from cultured cells using the RNeasy Mini Kit (Qiagen). Single-stranded cDNA was generated using the Superscript III first strand synthesis system (Invitrogen). The primers used for PCR are listed in Table S2.

Whole Mount Cornea Immunostaining. In order to highlight the corneal vasculature, mice were injected with FITC-dextran (2M molecular weight, Sigma) via the tail vein. Whole eyes were dissected and fixed immediately in 4%

paraformaldehyde (PFA) at 4^{o}C for 16 hours. Immunostaining was performed as described (*44*). Briefly, the entire cornea was washed in PBS for 1 hour, digested with proteinase K (20 µg/mL) for 5 min., permeabilized/fixed with 100% methanol for 30 minutes, and blocked in 1% blocking reagent (Roche) in Tris-buffered saline (TBS) for 16 hours at 4^{o}C. The FITC signal was amplified by incubating with 488-linked goat anti-FITC (Invitrogen) and then 488 donkey anti goat (Jackson ImmunoResearch). The complete cornea was then cut with three slits to make it flat on the slide and covered with a coverslip. Images were captured on a LSM-510 confocal microscope (Zeiss). CD45 immunofluorescence staining was performed using a rabbit anti-CD45 polyclonal antibody (Abcam) followed by biotin-labeled donkey anti-rabbit (Jackson ImmunoResearch) and Texas red-streptavidin (Vector Laboratories).

Subcutaneous Tumor Growth Models. 5x10^{5} cells from the CT26 parent or its subclones were injected subcutaneously into the right flank of syngeneic Balb/c mice. Celecoxib treatments (1000 mg/kg of chow, ad libitum, Pfizer) were initiated the next day, whereas axitinib (12.5 mg/kg body weight by daily gavage; Selleck Chemicals) and DC101 (40 mg/kg, three times per week, i.p. injection) treatments were initiated once the tumors reached approximately 100 mm^{3} in size. For the xenograft models, 3-5 million cells were injected subcutaneously into the right flank of nude mice. In these studies, axitinib was administered at 12.5 mg/kg body weight once daily by gavage, bevacizumab at 10 mg/kg body weight three times per week by i.p. injection, and celecoxib was provided in the

chow ad libitum (1000 mg/kg of chow). The celecoxib dose employed results in a mean concentration of celecoxib in the plasma of mice of 0.5 μg/mL (1.3 μM), which is similar to that found in human plasma after the usual 200-mg daily dose (*45*). Celecoxib (Celebrex) and bevacizumab (Avastin) were obtained from the NIH pharmacy. Treatments continued for the duration of the studies. Tumor size measurements were performed as previously descried (*4*). The formula used for calculation of tumor volume was: $V=[L\times W^2] \times 0.5$, where L is the length (longest tumor dimension) and W is the width (shortest tumor dimension).

Metastasis Models and Animal Imaging. Two models of metastasis were employed: an experimental liver metastasis model and a spontaneous breast cancer metastasis model. For experimental liver metastasis, $3x10^6$ luciferase-tagged HCT116-luc cells or $1x10^6$ CT26-luc cells were injected intrasplenically into athymic nude or syngeneic Balb/c mice, respectively. After 5 minutes (to allow liver seeding), spleens were resected and the abdomen sutured. *In vivo* bioluminescence imaging (IVIS Spectrum imager, PerkinElmer Inc.) was initiated 12-15 days after surgery. For the spontaneous breast cancer metastasis model, 1×10^6 4T1-luc cells were injected orthotopically into the right fourth mammary gland of Balb/c mice. Depending on the experiment, the primary tumor was resected either at 22 days (adjuvant studies) or when the tumors reached a size of 1000 mm^3. Treatment initiation also depended on the study: celecoxib and/or axitinib treatments were started either one day after primary tumor resection (adjuvant studies) or one day after tumor cell injection. Bioluminescence imaging

was used to quantify the extent of breast cancer metastasis 35 to 60 days after tumor cell injection, and again at the end of the study. Imaging was performed at peak luciferin uptake, approximately 10-12 minutes after D-luciferin (0.1 mL /20 g body weight) i.p. injection. Shortly before peak luciferin uptake, as determined by a dynamic scan on a subset of animals, mice were anesthetized in an induction chamber with 2.5-3% isoflurane at an oxygen flow rate of 1 liter per minute and then transferred to an imaging chamber, where the isoflurane was reduced to 2%. Exposure times of 1-5 min were utilized for metastasis imaging. Quantification of metastases (bioluminescence signal) was determined using the Living Image (version 4.3.1, PerkinElmer Inc.), implementing standard region of interests (ROI) drawn over the metastatic region. A Total flux threshold (photons/second) above a background was implemented in some comparisons to reduce variability among the subjects.

Blood Vessel Immunostaining and Quantification. Frozen sections were stained with anti-mouse CD31 (clone 390, eBioscience) followed by biotin-linked donkey anti-rat (Jackson ImmunoResearch) and Texas-red streptavidin. Sections were counterstained with DAPI and immunofluorescent images captured with a Zeiss LSM510 confocal microscope. At least 12 pictures per tumor and at least 3 tumors per group were analyzed. Free access Fiji software was used to calculate the blood vessel area using the formula: % area=total red signal/total DAPI signal.

Hematoxylin and Eosin (H&E) staining. Lungs were fixed in 4% PFA in PBS, routinely processed, and embedded in paraffin. Microtome sections were deparaffinized in xylenes, rehydrated, stained with H&E and imaged using an Aperio ScanScope XT.

Western Blotting. Antibodies recognizing total VEGFR2 or p-VEGFR2 were from Cell Signaling, while COX-2 antibodies were from Cayman Chemicals. For p-VEGFR2 detection from tumor tissues, VEGFR2 was immunoprecipitated using anti-VEGFR2 antibodies, and Western blotted with anti p-VEGFR2 (Tyr-1172). For detection of p-VEGFR2 in HMECs, cells were serum-starved for 8 hours, incubated with different concentrations of celecoxib or axitinib for 30 min or 16 h, and stimulated with VEGF (50 ng/mL) for 2 min. Cells were washed with ice-cold PBS, frozen immediately and lysed in TNT sample buffer containing 2 mM sodium orthovanadate prior to direct Western blotting. Western blotting was performed as previously described (*46*).

Myeloid Cell Analysis. Myeloid cells from spleens or subcutaneous tumor tissues (CT26 clone 3) were quantified by flow cytometry, double staining with FITC-linked anti-Gr1 and PE-linked anti-CD11b (BD Pharmingen). Briefly, tissues were minced with razors, incubated with 2 mg/mL collagenase A (Roche) in cell culture medium for 1 h at 37^{o}C with frequent agitation. The cell mixture was filtered through a 70 μM filter mesh, pelleted, resuspended in PBS and stained for 1 h at 4^{o}C prior to analyzing by flow cytometry (Becton Dickinson).

FIGURES

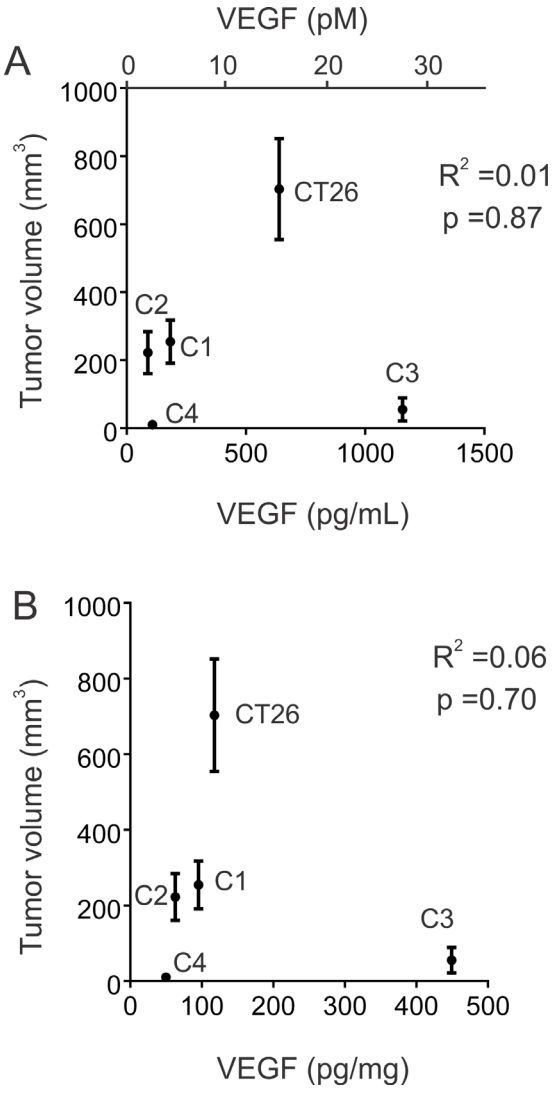

Fig. S1. Tumor volume does not correlate with VEGF expression in CT26 clones.

(A) Tumor volume 20 days after inoculation versus VEGF concentration in conditioned medium from CT26 parent cells or clone 1 (C1), C2, C3 or C4. VEGF concentrations are displayed as both molar (top X-axis) and mass values (bottom X-axis).
(B) Tumor volume 20 days after inoculation versus the amount of VEGF in tumors. The low R^2 value and high P value argue against a correlation. Pearson correlation calculations were two-tailed.

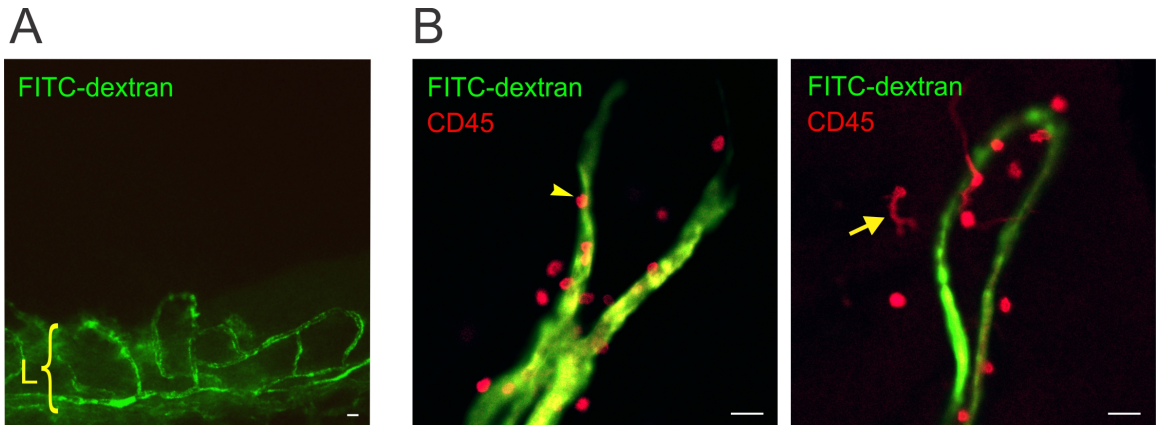

Fig. S2. CD45-positive inflammatory cells enter the cornea via newly formed vascular loops.

(A) The limbal vasculature (L) at the base of the cornea prior to tumor spheroid implantation and angiogenesis induction.
(B) After implantation of CT26 tumor spheroids into the avascular region of the cornea ~0.8 mm above the limbus, looping vessels from the limbal vasculature rapidly expanded into the cornea towards the tumor cells. CD45-positive inflammatory cells entered the cornea via the newly formed vascular loops. To visualize the functional vasculature in the cornea, FITC-dextran (green) was injected intravenously. Although sporadic CD45-positive dendritic cells were present throughout the cornea (arrow), CD45-positive leukocytes (red, spherical cells) were found closely associated with the new vascular loops that invaded the cornea. Some CD45-positive cells were found traversing the vessel wall (arrowhead). Bar=20 μm.

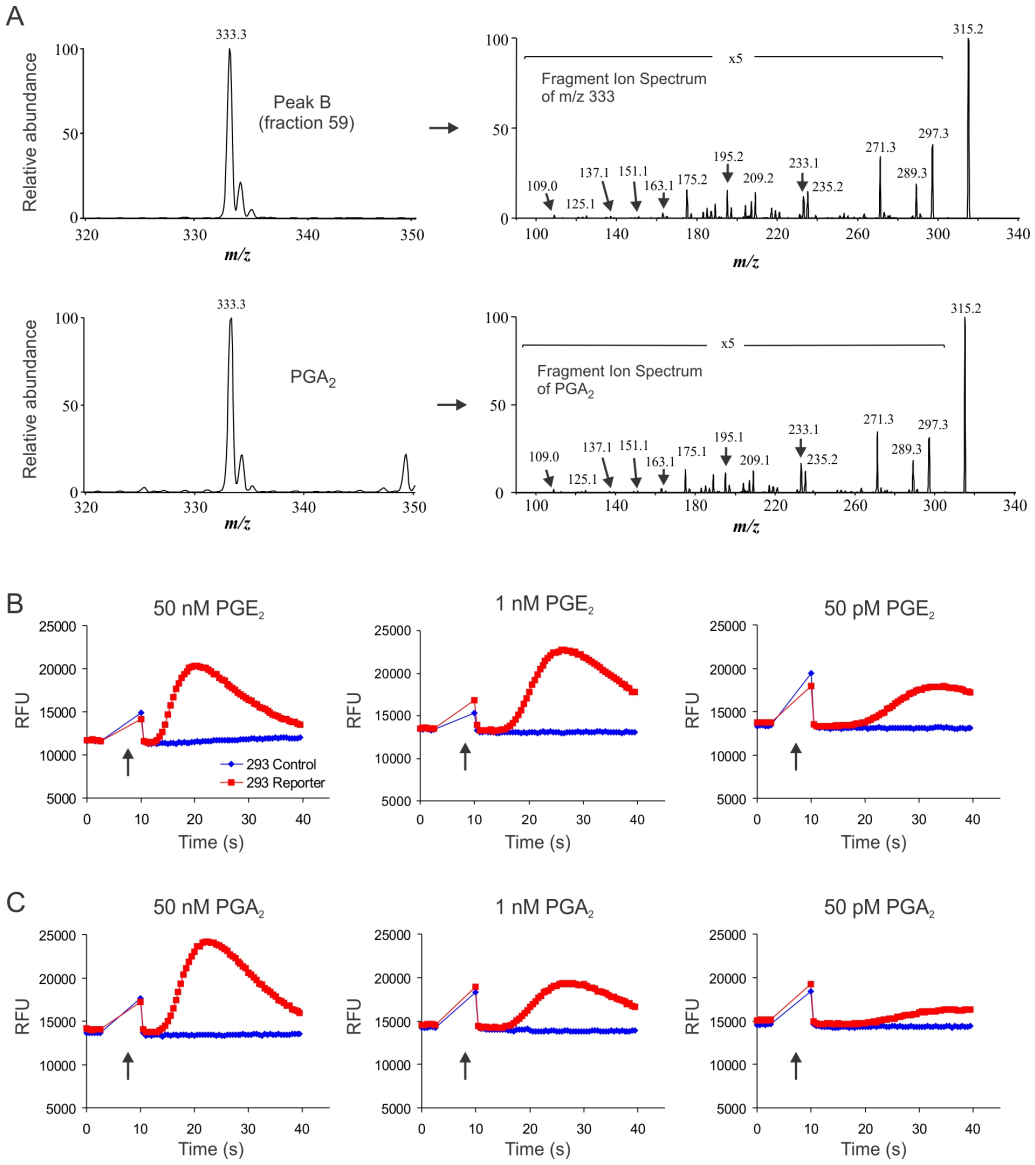

Fig. S3. PGE_2 and PGA_2 are the CT26-produced factors responsible for the calcium flux in reporter cells.

(A) Electrospray ionization mass spectrometry of fraction 60 from Peak B (see Fig 1 D and E) revealed a molecular species (m/z 333.3) and corresponding fragment ion spectrum (top panel) that was identical to pure PGA_2 (bottom panel). x5: A 5-fold zoom was applied to the ordinate in this region of the spectrum.
(B) Pure synthetically-produced commercial PGE_2 evoked a calcium flux in reporter cells but not control cells.
(C) Pure synthetically-produced commercial PGA_2 also evoked a calcium flux in reporter cells but not control cells. Arrow indicates injection time.

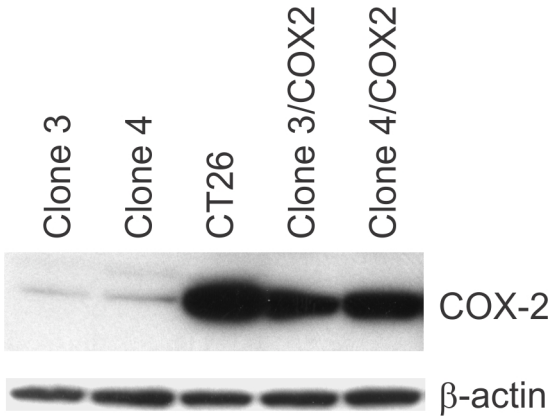

Fig. S4. Stable expression of *COX-2* in Clone 3 and Clone 4 results in elevated COX-2 protein expression.

Western blotting for COX-2 revealed that Clone 3 and Clone 4 cells stably transfected with *COX-2* (Clone 3/COX2 and Clone 4/COX2) expressed an amount of COX-2 that was similar to the endogenous amount found in the parent CT26 cell line. β-actin was used as a loading control.

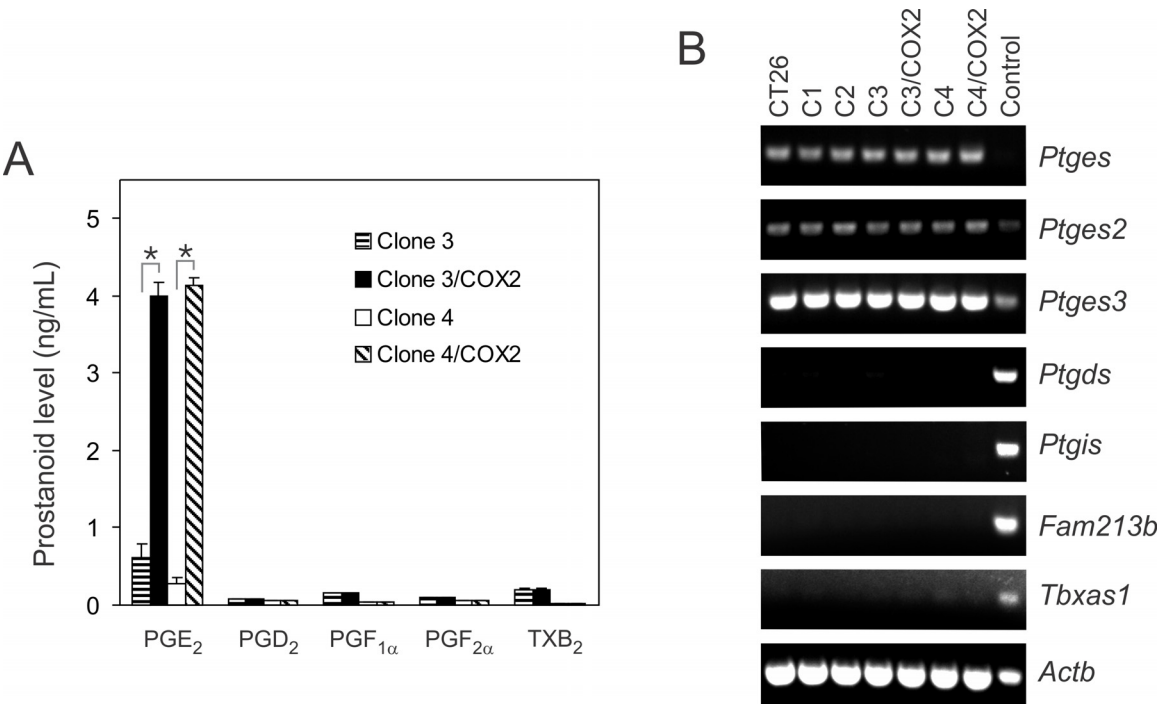

Fig. S5. COX-2 selectively upregulates PGE_2 without affecting prostanoid mRNA expression.

(A) Prostanoid concentrations were measured in the conditioned medium of cultured cells. PGE_2 was the only prostanoid that was significantly elevated in COX-2 overexpressing cells. *p<0.0001, Students T test.
(B) RT-PCR analysis was used to detect mRNA of each of the major prostanoid synthases in cultured CT26 clones. After 30 cycles of PCR, mRNA for each of the three PGE_2 synthases (*Ptges*, *Ptges2* and *Ptges3*) was readily detected, but prostaglandin D_2 synthase (*Ptgds*), prostaglandin I_2 (prostacyclin) synthase (*Ptgis*), prostaglandin F synthase (*Fam213b*), and thromboxane A synthase (*Tbxas1*) were undetectable. The positive control represents cDNA derived from a pool of normal adult brain, heart and lung tissues. β-actin (*Actb*) was used as a loading control.

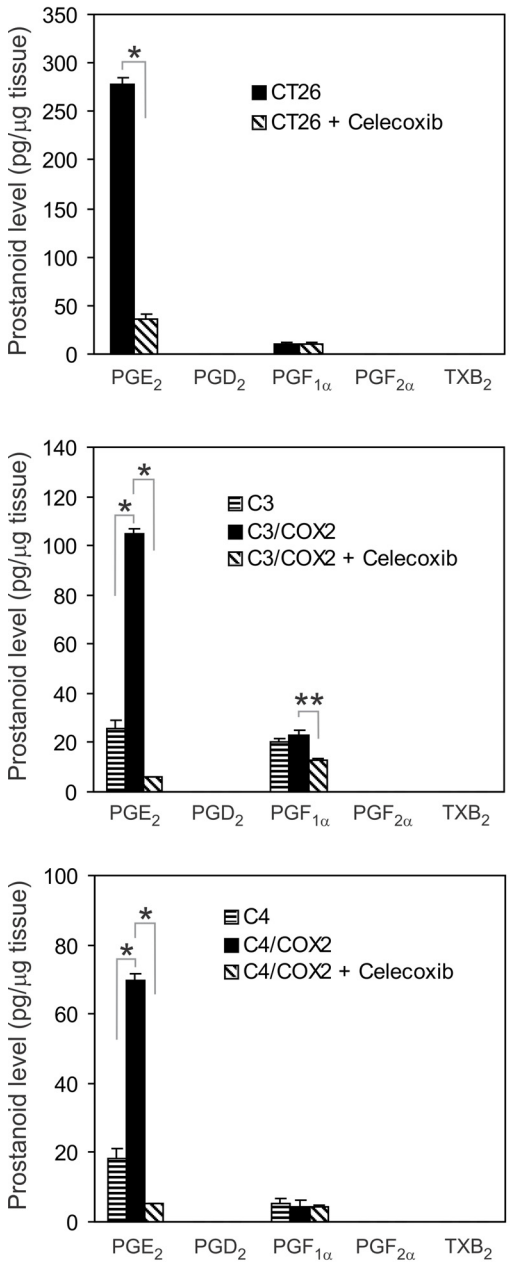

Fig. S6. COX-2 regulates PGE_2 expression in CT26 tumors *in vivo*.

An ELISA was used to measure prostanoid expression in CT26-derived tumors. Values were normalized to tissue weight. *p<0.0001. **p=0.01; Student's t-test (top panel) or ANOVA (middle and bottom panels).

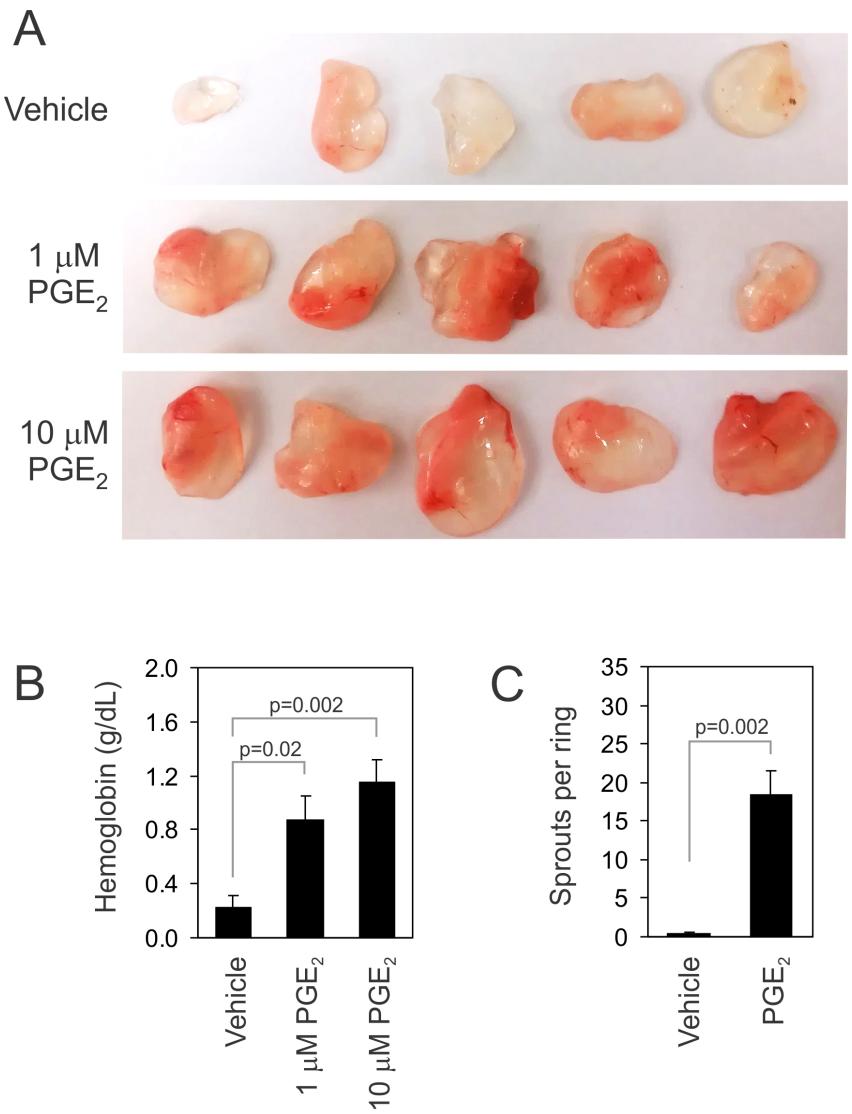

Fig. S7. PGE_2 stimulates angiogenesis *in vivo*.

(A) The Matrigel plug assay was used to evaluate PGE_2-induced angiogenesis *in vivo*. Plugs were removed and photographed 7 days after subcutaneous injection.
(B) Quantification of hemoglobin in the Matrigel plugs. N=5 per group.
(C) Addition of 75 nM PGE_2 to the culture medium resulted in an increased number of vessel sprouts in the aortic ring assay.
Data are presented as mean ± SEM.

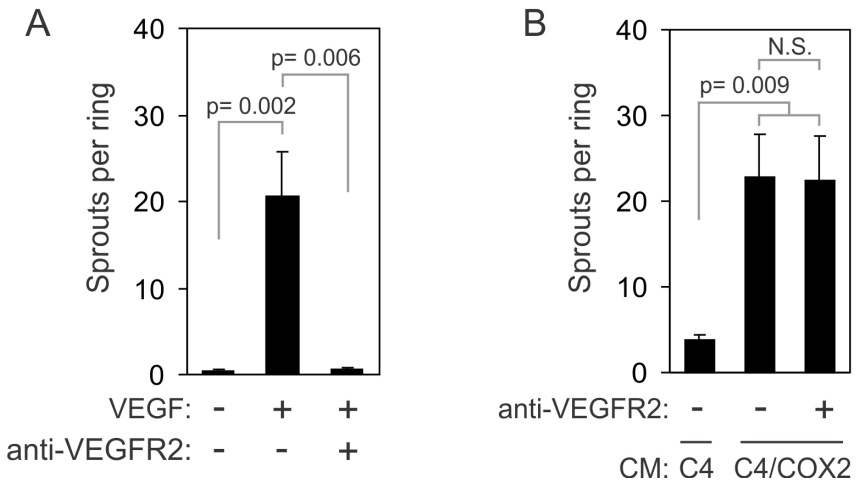

Fig. S8. Anti-VEGFR2 antibodies cannot block COX-2-induced angiogenesis.

(A) The aortic ring assay was used to assess the number of angiogenic sprouts induced by adding VEGF (20 ng/mL, 0.48 nM) to the basal culture medium. Sprouts were quantified 5 days after plating. DC101 anti-VEGFR2 antibodies (10 μg/mL, 63 nM) were able to block VEGF-induced angiogenesis.
(B) The aortic ring assay was used to assess the number of angiogenic sprouts induced by adding FBS-free EBM-conditioned medium (CM) from C4 or C4/COX2 into wells containing the aortic ring. Sprouts were quantified at day 5, and treatment with anti-VEGFR2 antibodies was the same as in *A*.
Data are presented as mean ± SEM. N.S.: Non-significant.

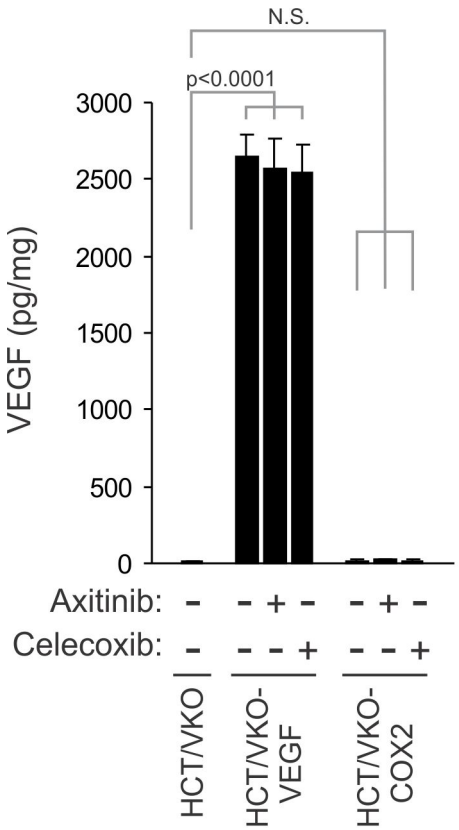

Fig. S9. HCT/VKO-VEGF tumors express a high amount of VEGF *in vivo*.

The amount of VEGF was significantly increased in HCT/VKO-VEGF tumors compared to parent HCT/VKO or HCT/VKO-COX2 cells. Axitinib and celecoxib treatment had no significant impact on the amount of VEGF in tumors.
Data are presented as mean ± SEM.

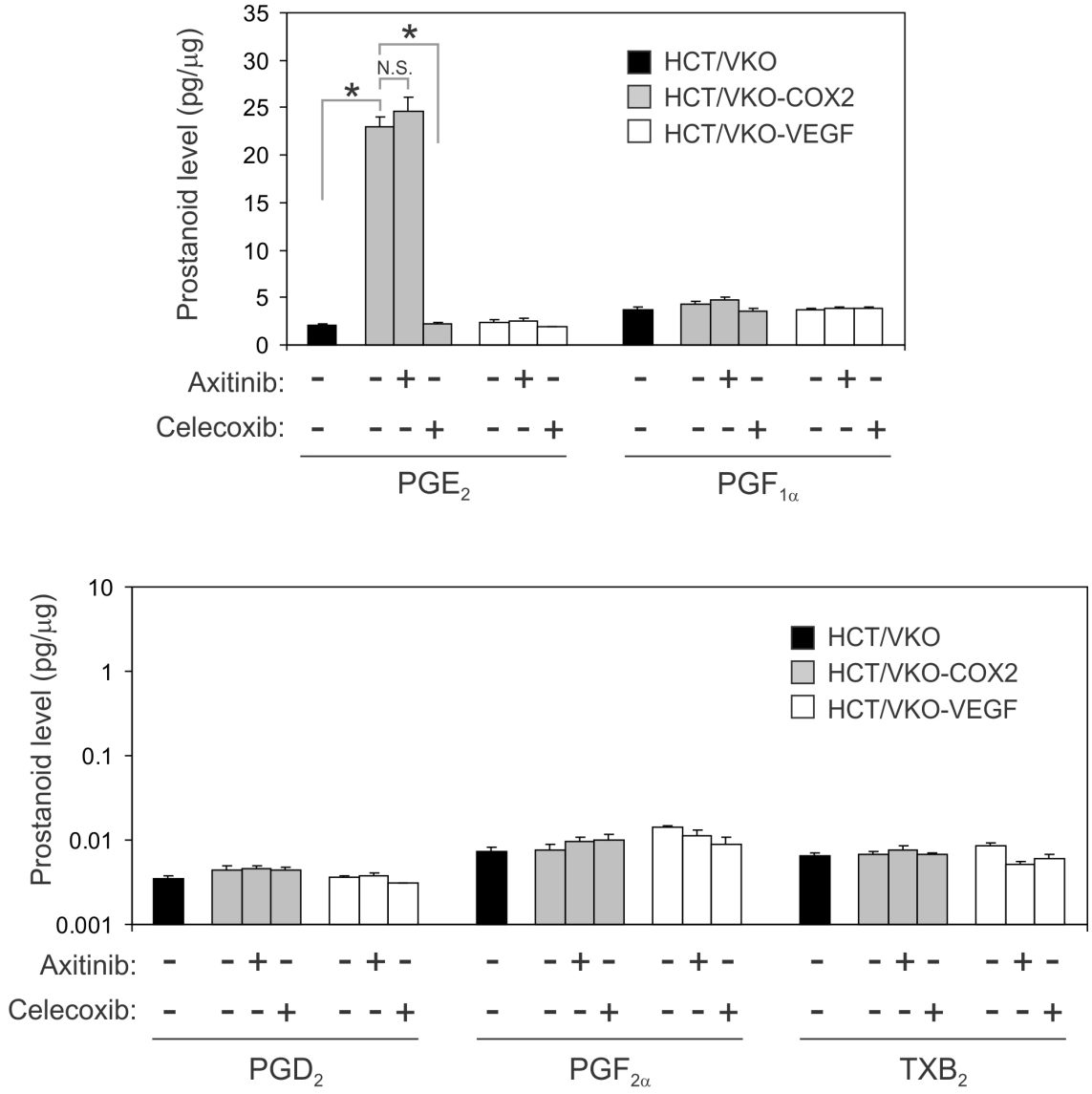

Fig. S10. COX-2 selectively regulates PGE_2 expression in HCT116 tumors *in vivo*.

Prostanoid expression was measured in HCT/VKO, HCT/VKO-VEGF and HCT/VKO-COX-2 tumors by ELISA. PGD_2, $PGF_{2\alpha}$, and TXB_2 expression levels were much lower than those of PGE_2 and $PGF_{1\alpha}$, but only PGE_2 amounts correlated with COX-2 activity. *P<0.0001. N.S. Non-significant. Data are presented as mean ± SEM.

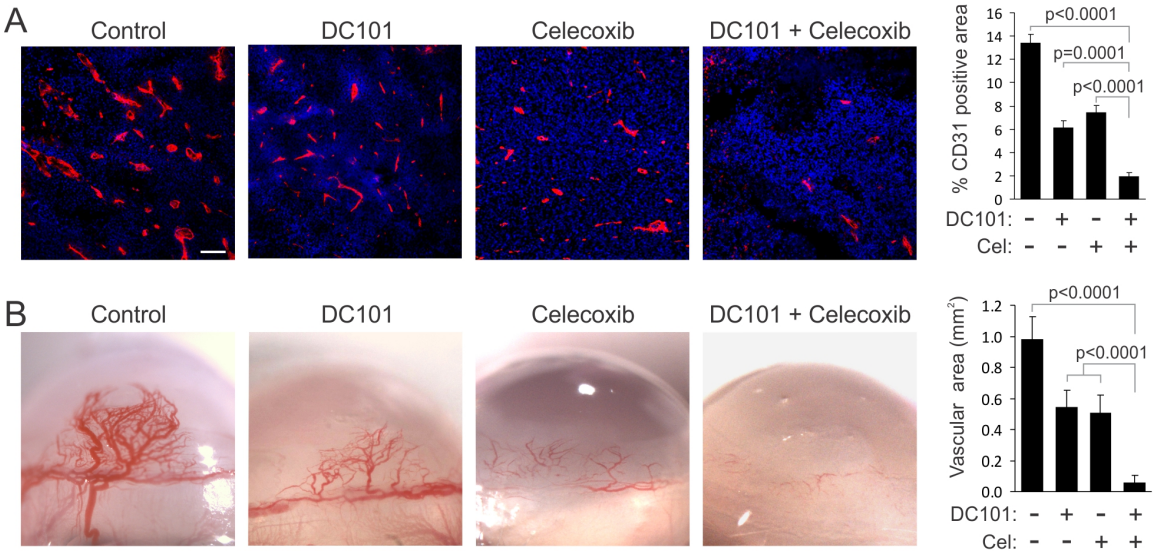

Fig. S11. Anti-VEGFR2 antibodies and celecoxib both reduce CT26-induced tumor angiogenesis.

(A) Immunofluorescence staining of CD31 (red) was used to assess blood vessel densities in CT26 tumors after treatment with anti-VEGFR2 antibodies (DC101) and celecoxib. Bar: 100 μm. Right panel: quantification of CD31 vessel staining. **(B)** The corneal assay was used to measure the effect of systemic treatment with DC101 and celecoxib on angiogenesis induced by CT26 tumor spheroids. Right panel: quantification of the corneal angiogenesis.
Data are presented as mean ± SEM.

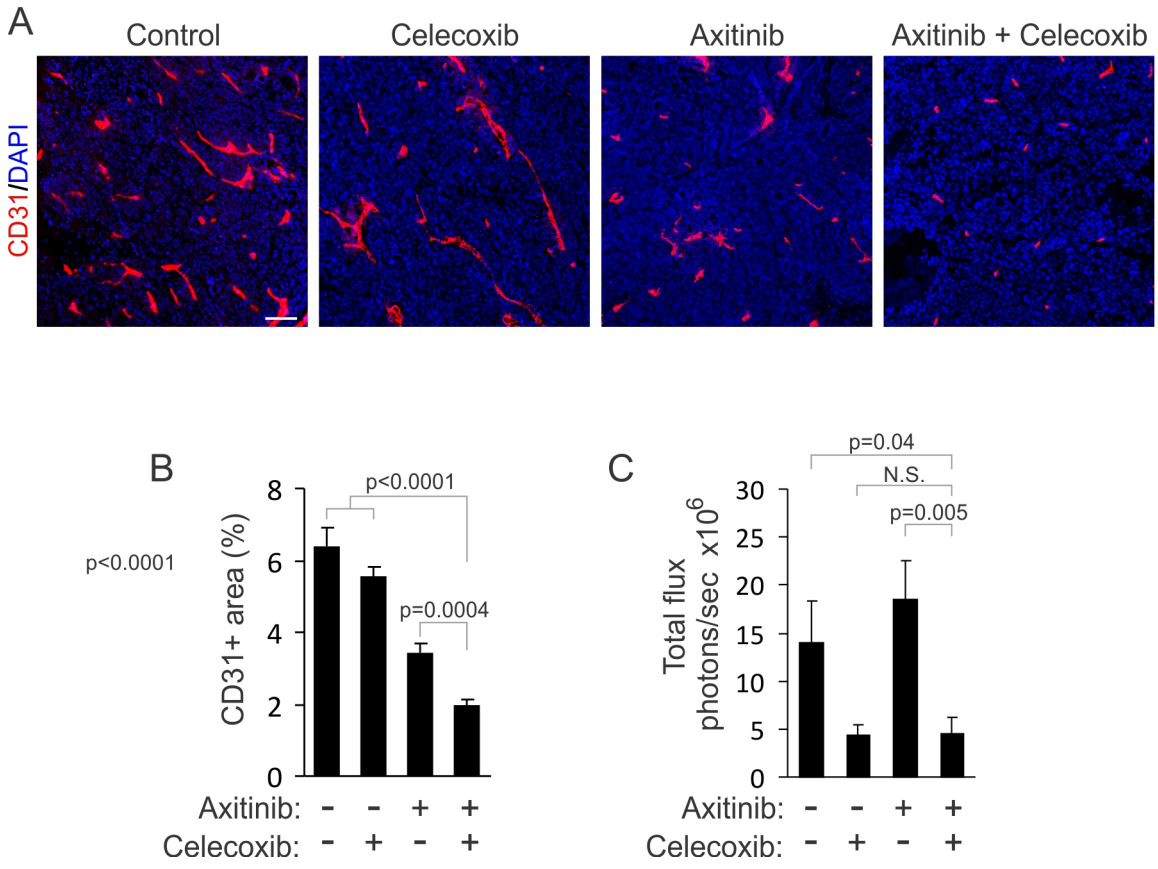

Fig. S12. VEGFR and COX-2 inhibition reduces tumor angiogenesis and blocks colon cancer metastasis.
(A) Immunofluorescence staining of CD31 (red) was used to assess blood vessel densities in HCT116 primary tumors after treatment with axitinib and celecoxib. Bar: 100 μm.
(B) Quantification of CD31 vessel staining in (*A*).
(C) *Ex vivo* quantification of CT26 tumors in mouse livers 2 weeks after intrasplenic injection of CT26-luc cells.
Data are presented as mean ± SEM.

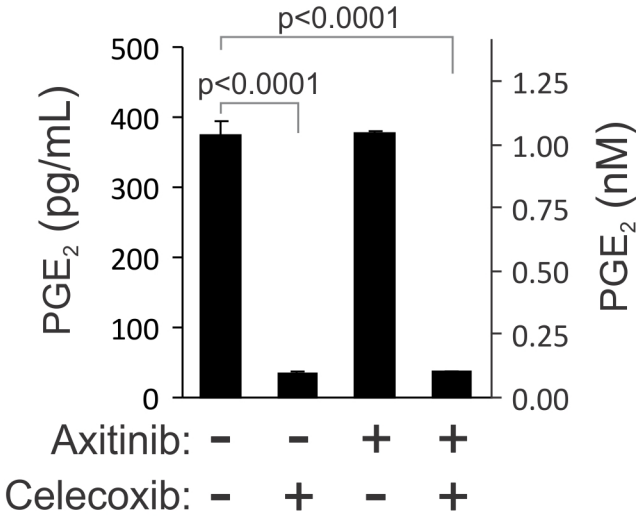

Fig. S13. PGE_2 expression is reduced in 4T1-luc cells after treatment with celecoxib.
An ELISA was used to measure PGE_2 concentration in the conditioned medium of cultured 4T1 cells before and after treatment with 10 nM axitinib or 25 μM of celecoxib. PGE_2 concentrations are displayed as both mass (left Y-axis) and molar (right Y-axis) values.
Data are presented as mean ± SD.

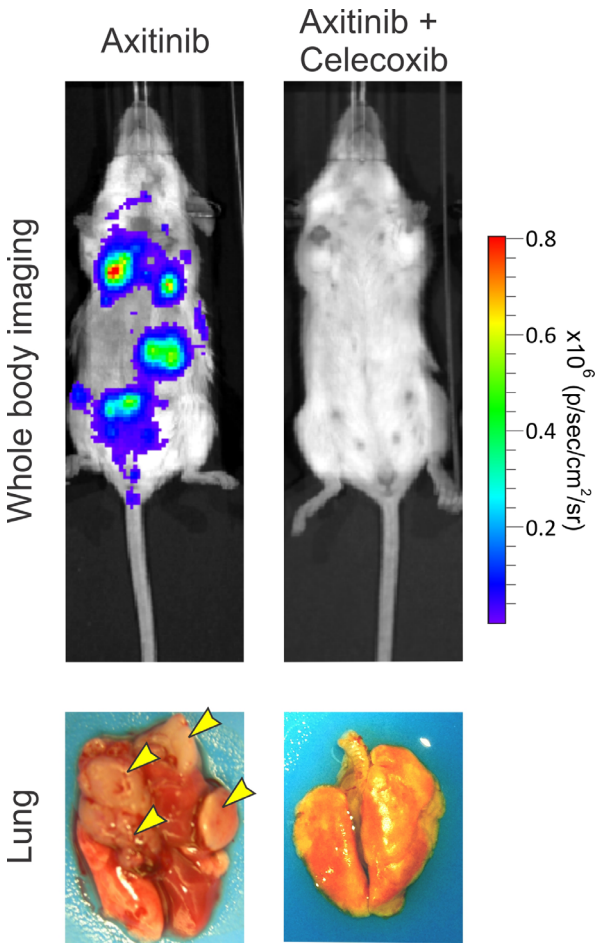

Fig. S14. Whole body luciferase imaging detects tumor burden in mice. Mice with high luciferase signals were found to have a large tumor burden upon histopathological analysis. In the example shown, the lung from an axitinib-treated mouse (left) contained multiple tumors (arrows). The mouse given the combined therapy (right) showed background luciferase signal and was alive and vigorous at the study end-point, 6 months after tumor cell inoculation. In survivors from this group, no evidence of tumor burden was found upon autopsy.

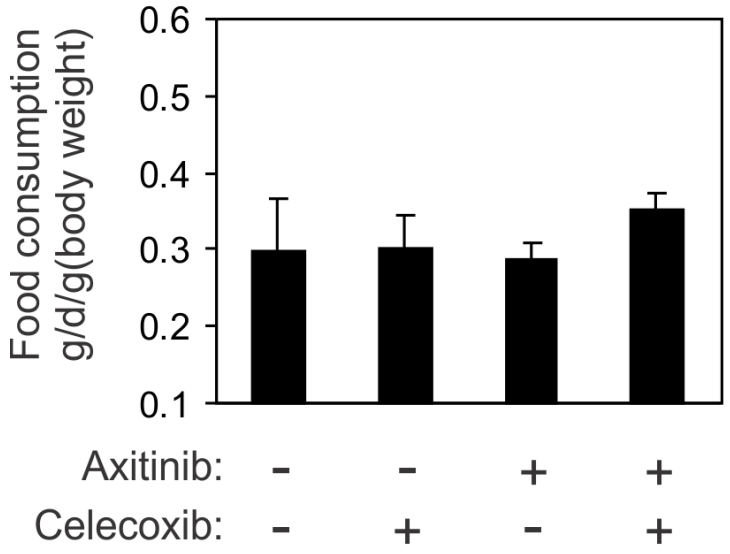

Fig. S15. Food consumption is unaltered in mice treated with axitinib and celecoxib.
After surgical removal of primary 4T1 tumors and randomization of mice into groups, food consumption was monitored for two weeks in control mice and in mice treated with axitinib, celecoxib, or both axitinib and celecoxib. Axitinib (12.5 mg/kg) was given daily by gavage, whereas celecoxib was provided in the feed (1000 mg/kg). Values represent the amount of food consumed per day per gram of body weight. Data are presented as mean ± SD. n=15 mice per group. No significant difference was found between any of the groups.

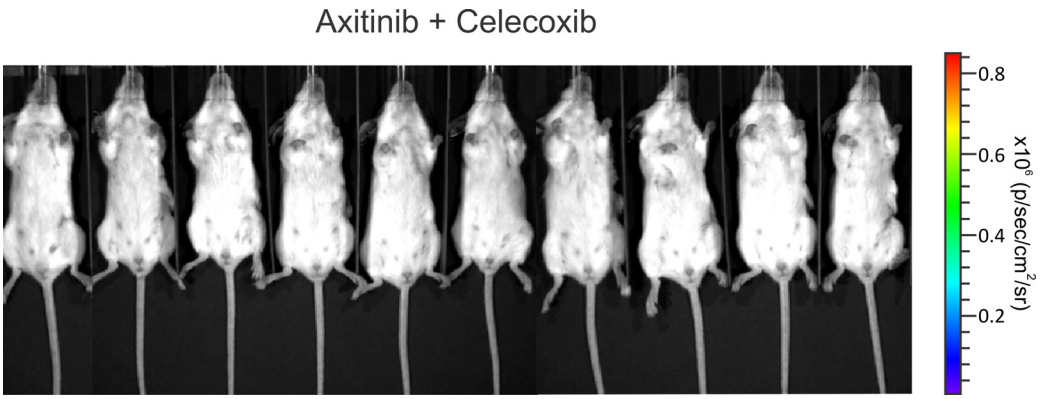

Fig. S16. Metastases are undetectable in long-term survivors treated with combined axitinib/celecoxib therapy.

Bioluminescence imaging failed to detect tumors in mice treated with both axitinib and celecoxib. In this adjuvant study, treatments began after tumors were surgically removed, and imaging was conducted 100 days after tumor cell inoculation.

Table S1. Original data for graphs that show composite results (provided as a separate Excel file).

Table S2. List of primers.

	Forward:	Reverse:
Ptges	CCAGATGAGGCTGCGGAAG	TTCAGCTTGCCCAGGTAGG
Ptges2	GGTGGAGGTGAATCCCGTG	TCCCGCCATACATCTGCTG
Ptges3	CAGTTGTCTTGGAGGAAGCG	CCATCATCTCAGAGAAACGGTC
Ptgds	TCCTGGGTCTCTTGGGATTC	AGTCTGGGTTCTGCTGTAGAGG
Ptgis	CTGCCAGCTTCCTTACCAGG	AGTCACCCAGCAGGACCG
Fam213b	ATGGTGTGCCGCTGGATC	AGCTGTTGTACCGCTTGAAGC
Tbxas1	TGCTTCCACCTTCTGTATCCC	ATGTCAAAGCCTTCCACGC
Actb	CACCCGCCACCAGTTCG	AAGGTCTCAAACATGATCTGGG